ISSN 1855-9913

Journal of the Laser and Health Academy
Vol. 2018, No.1; www.laserandhealth.com

Dual Tissue Regeneration: Non-Ablative Resurfacing of Soft Tissues with FotonaSmooth® Mode Er:YAG Laser

Matjaz Lukac[1], Adrian Gaspar[2], Franci Bajd[3]
[1]Institut Jozef Stefan, Jamova 39, 1000 Ljubljana, Slovenia
[2]Espacio Gaspar Clinic, Mendoza, Argentina
[3]University of Ljubljana, Faculty of Physics and Mathematics, Jadranska 19, 1000 Ljubljana, Slovenia

ABSTRACT

It is shown that the extraordinary, extremely short optical penetration depth of the Er:YAG laser in tissue water makes this laser not only optimal for ablative procedures, but also for non-ablative resurfacing. A process of fast heat shocking of the epithelium, in addition to slow thermal injury of the connective tissue, is involved in non-ablative FotonaSmooth® mode Er:YAG resurfacing procedures. This dual tissue-regeneration mechanism (DTR) is accessible only to thermal remodeling devices with an extremely short energy penetration depth within the tissue, using unique FotonaSmooth® mode pulsing characteristics. In this regard, the Er:YAG laser wavelength holds a unique position due to its extraordinary wavelength coinciding with the highest absorption peak of water at 2,940 nm. It is proposed that this unique characteristic of the Er:YAG laser contributes significantly to the reported safety and efficacy of the FotonaSmooth® Er:YAG skin tightening, thermotherapy for treating genitourinary syndrome of menopause, and thermotherapy of snoring and sleep apnea.

Key words: Er:YAG resurfacing, non-ablative thermotherapy, smooth mode, FotonaSmooth mode, syndromes of menopause, variable heat shock

Article: J. LA&HA, Vol. 2018, No.1; pp. 1- 15.
Received: July 17, 2018; Accepted: September 10, 2018.

I. INTRODUCTION

Laser treatment methods for combating symptoms of tissue aging involve two basic laser modalities for tissue rejuvenation: ablative and non-ablative laser resurfacing of soft tissues (See Fig. 1) [1].

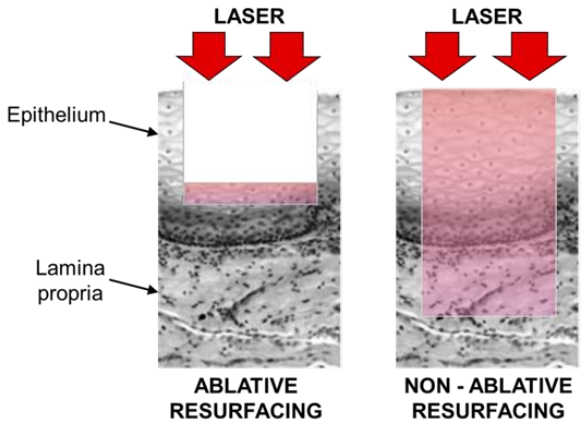

Fig. 1: Ablative and non-ablative resurfacing of soft tissue. Thermally affected tissue is colored in red.

It is important to note that it is not the laser type or the laser wavelength (λ) that determines whether a resurfacing procedure is non-ablative or ablative, but the laser pulse duration and fluence F (in J/cm^2), i.e., the energy of a laser pulse delivered to the tissue surface within the laser beam spot area [2-4]. Therefore, the mid-IR lasers such as Er:YAG (λ = 2,940 nm) and CO_2 (10,640 nm) lasers, which are often considered as "ablative lasers" due to their history of being used very successfully to perform ablative resurfacing [2,5], can be and have also been successfully used to perform non-ablative procedures [6-10]. This applies especially to the Er:YAG laser technology, which is capable of delivering a wide range of fluences and pulse durations [2].

In laser resurfacing procedures performed with mid-IR lasers, it is the tissue's water content, not its pigment that plays the role of an absorbing chromophore. In these "bulk tissue" treatments, the temperature elevation ΔT is not limited to a particular pigment, such as melanin or hemoglobin, but to the superficially irradiated tissue layer with its thickness determined by the laser's optical penetration depth (δ) and the subsequent thermal diffusion [2-4].

Ablation occurs when the maximal tissue temperature (T_{max}) during a laser pulse reaches the ablation temperature T_{abl}. The ablation results from

micro-explosions of overheated tissue water within the elastic tissue [3]. Since the water contained within the confined solid tissue cannot expand freely, the ablation temperature is not at the boiling temperature of water under atmospheric pressure of about 100 °C but at a much higher temperature of $T_{abl} \approx 250$ °C [3, 11].

As shown in Fig. 2, it is the clinician's choice of laser fluence that determines whether a resurfacing procedure will be non-ablative or ablative. For fluences below the ablation threshold, the maximal tissue temperature T_{max} grows approximately linearly with fluence. The maximal temperature increases with laser fluence until the ablation threshold fluence F_{abl} is reached, at which point the maximal temperature achieves the ablation ("boiling") temperature T_{abl}. For fluences above F_{abl}, the maximal temperature remains fixed at T_{abl}, similarly to the case of boiling water that keeps its temperature at 100 °C regardless of the heating power.

Since the Er:YAG laser wavelength is limited to it's very shallow optical penetration depth [2], it has been hypothesized that instead of having to rely on the FotonaSmooth® mode heat pumping technique [6-10], devices with a deeper penetration depth may represent an equivalent alternative for thermal remodeling [56]. However, the extraordinary clinical results obtained with the FotonaSmooth® mode Er:YAG laser, with a small number of reported complications, indicate that there may be an additional mechanism of action involved that makes the Er:YAG laser wavelength particularly suitable for non-ablative resurfacing procedures.

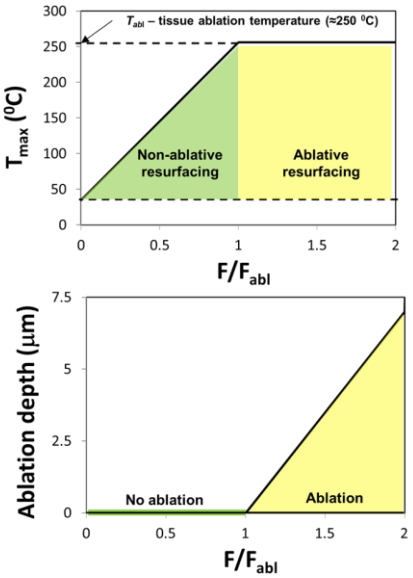

Fig. 2: Dependence of the tissue surface temperature (above) and the ablation depth (below) on the resurfacing laser's pulse fluence F. Non-ablative procedures are performed with fluences $F < F_{abl}$. Ablative procedures start at fluences above the ablation threshold fluence F_{abl} (i.e., when $F/F_{abl} = 1$) characterized by $T_{max} = T_{abl}$.

This article examines the extraordinary aspects of non-ablative resurfacing with the FotonaSmooth® Er:YAG laser, representing a mid-IR laser with the highest absorption in tissue water. The principles detailed here provide a framework for understanding the treatment protocols and mechanisms of action involved in FotonaSmooth® mode Er:YAG laser non-ablative soft-tissue regeneration procedures [6, 13].

II. MATERIALS AND METHODS

a) Er:YAG laser

The Er:YAG laser wavelength coincides with the absorption peak of water at 2,940 nm. This makes the Er:YAG laser unique since it has the highest absorption in soft tissues in comparison to any other medical laser within a broad range of wavelengths from λ = 200 nm – 1 mm (see Fig. 3) [2].

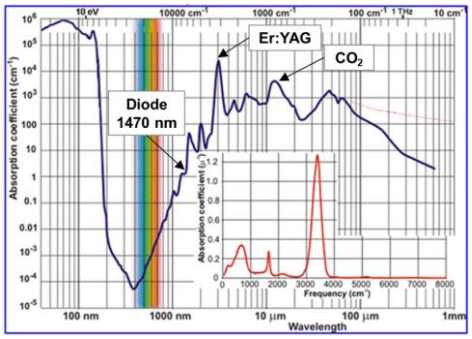

Fig. 3: Absorption coefficient in tissue water as a function of laser wavelength. The highest absorption in water is at the wavelength of 2,940 nm, which coincides exactly with the wavelength of Er:YAG laser radiation.

The Er:YAG laser wavelength is therefore selectively highly absorbed by tissue water, with an energy penetration depth of only about $\delta \approx 1$ μm. In comparison, the penetration depth of the next most highly absorbed laser, the CO_2 laser, is about 20 μm. As will be shown further below, the unique, extremely short penetration depth of the Er:YAG laser makes this laser exceptional when it comes to the safety and efficacy of non-ablative tissue regeneration procedures.

b) Er:YAG laser non-ablative resurfacing

The experimentally obtained Er:YAG laser ablation threshold fluence on soft tissues depends slightly on the pulse duration (it is higher for longer pulse durations), and ranges from 1.5 to 2.2 J/cm² [2, 12, 14, 15]. Therefore, the resurfacing of soft tissues with Er:YAG laser fluences below or equal to 1.5 J/cm² can be considered to belong to the non-ablative treatment category.

The Er:YAG laser wavelength has been used for non-ablative and ablative resurfacing procedures for over 20 years. For example, the Er:YAG laser is currently cleared by the US FDA for the resurfacing of all soft tissues [16], including skin and mucous membrane, with fluences in the range of F = 0.6 – 4 J/cm², and repetition rates in the range of f = 6-20 Hz. Similarly, Er:YAG laser has been cleared by the US FDA for indications in gynecology and genitourology, with fluences in the range of F = 0.8 – 3.2 J/cm², and repetition rates in the range of f = 8-20 Hz. For both groups of indications, the cleared fluence range covers both non-ablative and ablative procedures (see Fig. 4).

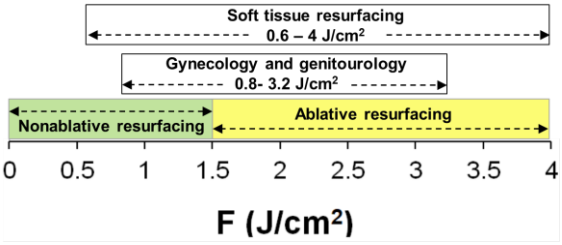

Fig. 4: Er:YAG laser fluences for soft-tissue resurfacing and gynecological and genitourinary indications. The fluence range covers both the non-ablative and ablative resurfacing modality, with the ablation threshold fluence of $F_{abl} \approx 1.5$ J/cm² separating the two modalities.

As opposed to ablative resurfacing where the epithelium gets ablated, non-ablative resurfacing uses a thermal approach to induce only a remodeling of epithelial and connective tissues without obvious epithelial injury (see Fig. 5) [1,2,6]. The mechanism of action is based on thermally injuring [17-19] the tissue in order to cause a reactive inflammatory response, resulting in an increase of the biosynthetic capacity of fibroblasts and other cells, inducing the reconstruction of an optimal physiological environment, the enhancement of cell activity, hydration, and the synthesis of collagen and elastin [20].

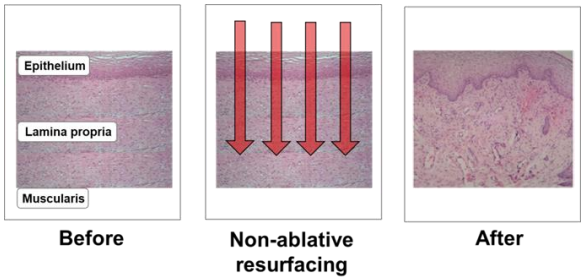

Fig. 5: The goal of non-ablative resurfacing procedures is tissue regeneration. Histological pictures depict the vaginal mucosa before and after a non-ablative Er:YAG laser procedure [21], showing the regeneration of the epithelium and lamina propria. Mucous tissue is depicted; however the figure applies also to skin [89].

c) Thermal exposure time

A thermal injury may occur when tissue cells are exposed to a thermal pulse, i.e., to an elevated temperature $T = T_0 + \Delta T$ for a certain duration of exposure. When using an energy-based medical (EMD) device such as a laser or a radiofrequency or an ultrasound device to create a thermal pulse within a tissue, the shape of the generated temperature pulse typically does not follow the duration (t_{in}) and the temporal shape of the delivered energy pulse. The thermal pulse consists of a temperature ramp-up heating phase during which the temperature reaches its maximal value (T_{max}), and a temperature ramp-down cooling phase during which the temperature returns back to its initial temperature T_0 [3]. The heating phase lasts for approximately the duration of the energy pulse (t_{in}), while the cooling phase is determined predominantly by the rate of the heat flow away from the heated tissue volume (see Fig. 6). This is because once the tissue is heated up, its temperature persists also after the energy pulse has ended. The temperature remains high until the tissue is cooled down by the process of heat conduction into the surrounding colder volume. It is therefore the thermal conduction process rather than the energy pulse duration itself which typically sets the lower limit to the achievable duration of a thermal pulse [3,11].

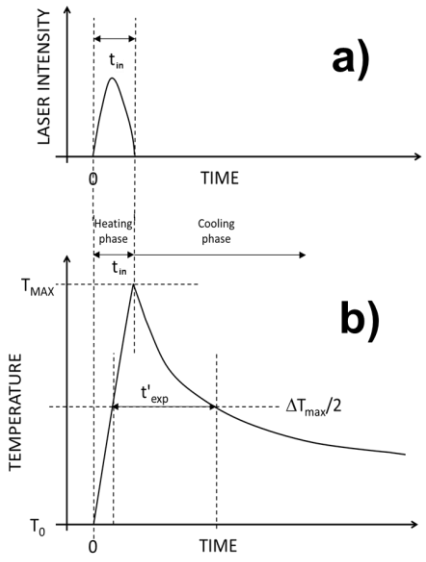

Fig. 6: The duration of a thermal pulse t'_{exp} is determined by (a) the duration of the laser pulse and (b) the duration of the cooling phase during which the heated up tissue cools down by means of relatively slow heat conduction.

d) Arrhenius model of thermal injury

The physical process of thermodynamically heating the tissue during a thermal pulse is accompanied by the chemical process of protein denaturation as a result of the cellular exposure to the increased temperature [17].

A commonly used metric for tissue damage (Ω) is the ratio of the concentration of native (undamaged) tissue before thermal exposure (C_0) to the concentration of native tissue at the end of the exposure time (C_f). The tissue damage is then calculated using the Arrhenius damage integral calculated over the time of the thermal exposure [17,22,23]:

$$\Omega = \ln\frac{C_0}{C_f} = A\int exp\frac{-E}{RT_{(t)}}dt \ . \qquad (1)$$

Here, A is the frequency factor, i.e. the damage rate (in s^{-1}) and E is the activation energy [in J/kmol] of the biochemical process responsible for the tissue denaturation. The parameter R is the gas constant (R = 8.31 x 10^3 J/kmol K).

As can be seen from Eq. 1, the tissue injury grows exponentially with the elevated temperature, and linearly with the time of exposure. The tissue damage kinetics is commonly characterized by a critical (i.e., damage threshold) temperature (T_{crit}), representing the temperature at which the concentration of the undamaged tissue is reduced by a factor of e (i.e., when Ω = 1). Assuming a single biochemical damage process and a square-shaped temperature pulse with a constant temperature during the thermal exposure time (t_{exp}), the critical temperature is defined by [7, 9]:

$$T_{crit} = \frac{E}{R \times \ln(A \times t_{exp})} \qquad (2)$$

As an example, Fig. 7 shows the dependence of the critical temperature on the exposure time t_{exp} for a single biochemical process with A = 4.7 x 10^{89} s^{-1} and E = 5.67 x 10^8 $Jkmol^{-1}$.

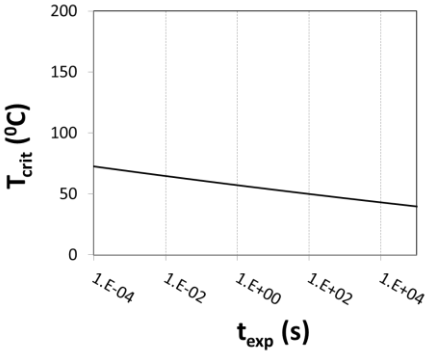

Fig. 7: Dependence of the critical temperature on exposure time for a single biochemical process with A = 4.7 x 10^{89} s^{-1} and E = 5.67 x 10^8 $Jkmol^{-1}$.

For the same exemplary single biochemical process, Fig. 8 shows the dependence of the percentage of the remaining undamaged cells on temperature for a thermal pulse with t_{exp} = 1 s.

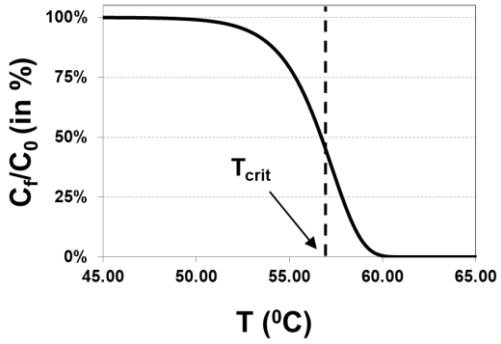

Fig. 8: Percentage of undamaged cells following a thermal pulse with t_{exp} = 1 s, as a function of temperature T for a single biochemical process with A = 4.7 x 10^{89} s^{-1} and E = 5.67 x 10^8 $Jkmol^{-1}$.

Studies of tissue damage dynamics demonstrate that when considering extremely short and long exposure times, cell viability cannot be described by a single biochemical process [17, 24-33]. For example, measurements of damage threshold temperatures at extremely short exposure times (commonly present during Er:YAG laser treatments) exhibit a shift to temperatures which are much higher than what would be expected from a single biochemical process characterizing the damage dynamics at long exposure times [30-32].

A description of the measured dependence involves a more complex, VHS (Variable Heat Shock) response model [11], which takes into account the observed deviation from the single-process Arrhenius relation by assuming that the cell viability can be described as a combined effect of two biochemical processes that dominate cell survival characteristics at very short and very long exposure times (See Fig. 9).

In the VHS model, the effective VHS (Variable Heat Shock) damage integral Ω_{VHS} is calculated from the combined effect of the damage integrals $\Omega_1(t_{exp})$ and $\Omega_2(t_{exp})$ belonging correspondingly to the processes 1 and 2, as follows [11] :

$$\left(\frac{1}{\Omega_{VHS}}\right)^p = \left(\frac{1}{\Omega_1}\right)^p + \left(\frac{1}{\Omega_2}\right)^p \qquad (3)$$

Here, p is the transition coefficient that determines the transition between the two limiting processes. For the VHS critical temperature curve shown in Fig. 9, the transition coefficient is equal to p = 0.16, with the long exposure time process 1 characterized by A_1 = 4.7 x 10^{89} s^{-1} and E_1 = 5.67 x 10^7 $Jkmol^{-1}$, and the short exposure time process 2 characterized by A_2 = 1.45 x 10^4 s^{-1} and E_2 = 1.03 x 10^7 $Jkmol^{-1}$ [11].

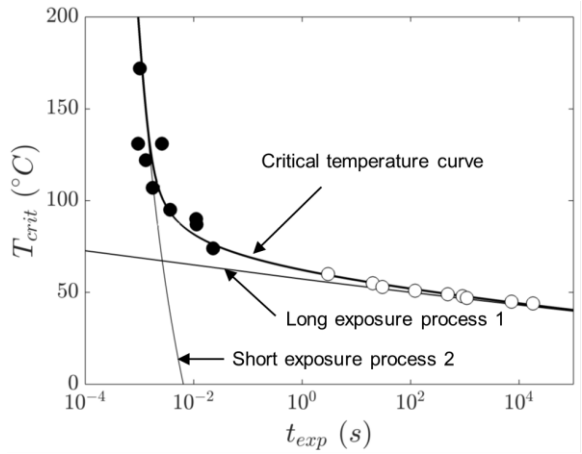

Fig. 9: Dependence of the measured critical (damage threshold) temperatures T_{crit} on the duration of thermal exposure t_{exp}, together with the critical temperature curve according to the VHS model, representing the combined effect of two limiting biochemical processes that define cell viability at extremely long and extremely short exposure times. Full circles represent published measured values for short exposure times [30-31] and open circles represent measured critical temperatures for long exposure times [17, 19].

III. RESULTS

a) Dual tissue-regenerative erbium

The human body consists of several types of tissue, among them the epithelial and connective tissues (see Fig. 5). Epithelial tissue covers most of the internal and external surfaces of the body and its organs. The type of epithelial tissue that lines various cavities in the body, such as the mouth or vagina, and covers the surface of internal organs is known as the mucous membrane or mucosa. Another type of epithelial tissue is the epidermis, which covers the skin surface. The principal cell type that is found in the epithelia are keratinocytes, which generate biomolecules necessary for the stability and resistance of the epithelial layer to mechanical stress. The connective tissue, such as the skin's dermis or vaginal lamina propria, lies below the epithelial tissue and helps to hold the body together. The cells of connective tissue include fibroblasts, adipocytes, macrophages, mast cells and leucocytes. Fibroblasts are the most common cells of connective tissue. A fibroblast is a type of cell that synthesizes the extracellular matrix and collagen, the structural framework (stroma) for human tissues, and plays a critical role in wound healing.

The clinically observed regenerative effect of non-ablative resurfacing procedures with the FotonaSmooth® mode Er:YAG laser can be explained by the effect of two combined mechanisms of action involving both biochemical processes, the long exposure process 1 and the short exposure process 2. The two mechanisms involved in this Dual tissue-Remodeling Mechanism (DTR) are (see Fig. 10):

i) Relatively slow thermal injury to connective tissues involving the long exposure biochemical process 1;
ii) Fast heat shocking of the epithelium involving the short exposure biochemical process 2, and subsequent triggering of regeneration of deeper lying tissues.

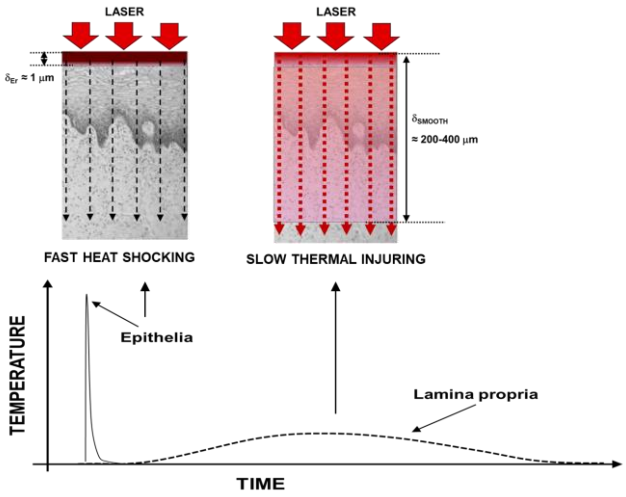

Fig. 10: Dual tissue-remodeling mechanism (DTR) involved in non-ablative resurfacing with FotonaSmooth® mode Er:YAG laser. The initial, very short temperature pulse as generated at the epithelial surface by the highly absorbed Er:YAG laser is transformed via heat diffusion into a long lasting thermal pulse within the deeper lying connective tissue. As a result there are two complementary regenerative processes initiated during tissue resurfacing: i) an indirect triggering effect by short duration heat shocking of the epithelium (left); and ii) direct slow thermal injury of the connective tissues (right).

b) Direct, slow process-based regeneration

Since it is the connective tissue that is responsible for holding the skin, vagina and other organs together, non-ablative laser rejuvenation procedures typically focus on the regeneration of connective tissues (see Fig. 5) [1, 34]. The mechanism responsible for the promotion of collagen production is the direct thermal injury of the connective tissue leading to an inflammatory response [20]. The inflammation of the connective tissue attracts cells such as neutrophils and macrophages to the site of injury, which in turn release growth factors and cytokines responsible for repair.

It should be noted that even for very short laser pulse durations the thermal exposure times involved in heating of connective tissues are long, on the order of seconds or longer. This is because the laser-heated connective tissue remains heated for a long time, owing to the weak heat flow from the relatively large heated volume to the surrounding unheated tissue [3].

The long exposure times limit the maximal direct regeneration temperatures to below $T_{crit} \approx 55 - 70$ °C, as defined primarily by the long exposure biochemical process 1 (See Fig. 9).

The technique employed in heating deeper lying tissues with the superficially absorbed Er:YAG laser consists of delivering laser energy using a special FotonaSmooth® mode (see Fig. 11), consisting of a sequence of consecutively delivered sub-ablative laser pulses following each other with a repetition rate of f = 10 – 20 Hz [6-10, 13, 34], which is within the US FDA cleared range of frequencies for Er:YAG soft-tissue resurfacing.

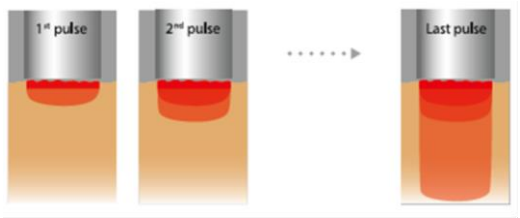

Fig. 11: The Er:YAG laser's FotonaSmooth® mode consists of a series of sub-ablative micro pulses, effectively "pumping" the heat away from the surface deeper into the tissue.

The FotonaSmooth® mode sequence effectively "pumps" the laser generated heat by means of heat diffusion away from the epithelia, several hundred microns deep into the connective tissue (see Fig. 12) [2, 34, 35]. Non-ablative FotonaSmooth® mode resurfacing with Er:YAG laser thus results in a controlled thermal injury of the dermis or lamina propria without any ablation of the epithelium and without any damage to the underlying fibromuscular tissue.

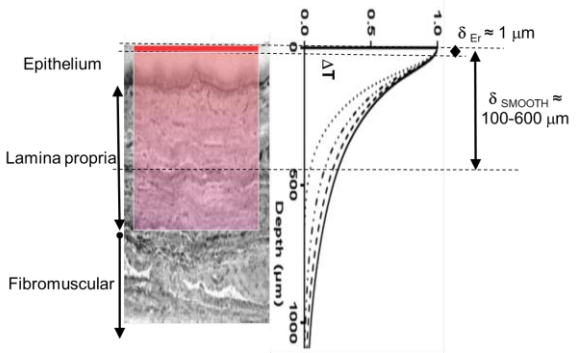

Fig. 12: With the FotonaSmooth® Er:YAG mode, the tissue is heated up to the depth of δ_{SMOOTH} = 100-600 μm. It is not the optical penetration depth δ_{Er} but the heat penetration depth δ_{SMOOTH} which determines the depth of the thermally modeled tissue. Mucous tissue is depicted; however the figure applies also to skin [89].

Numerical calculations of the FotonaSmooth® mode Er:YAG laser exposure show an increase in temperature to depths of up to 400 μm, resulting in collagen denaturation within the depth of about 200 μm [2, 3, 34, 37]. In studies on rat skin, dermal collagen coagulation to a depth of approximately 250 μm was reported [35, 36]. And in a study on eyelid skin of volunteers with blepharochalasis, remodeling and myo-fibroblast proliferation at tissue depths of up to 240 μm were observed at day 21 after the FotonaSmooth® mode Er:YAG laser treatment [7].

c) Indirect, fast process-based regeneration

It is to be noted that for most resurfacing devices it represents a considerable challenge to heat up the deeper lying connective tissue to sufficiently high temperatures. This is because in order to reach the fibroblasts, the delivered energy must first traverse the epithelial layer located above the basement membrane. This means that the delivered energy may be predominantly absorbed by the superficial layers. Accordingly, the maximal allowed temperatures that apply to the epithelial layer limit the temperatures that can be generated within the connective tissue. In many cases, the physician is thus faced with a trade-off between using enough energy for effective therapy while staying within the thresholds for damage to the superficial tissue.

However, as can be concluded from Fig. 9, the barrier represented by the maximal allowed epithelium temperature can be overcome, provided that the epithelium is exposed to high temperatures for only a very short time. For very short exposure times (t_{exp} < 0.01s) the epithelia can be heated to temperatures much higher than 65 °C, and under appropriate conditions even up to T_{abl}, without any significant biochemical injury.

It is in this regime that the advantage of the Er:YAG laser's short penetration depth becomes most evident. Namely, in order for the cooling phase of a heat shock thermal pulse (see Fig. 6) to be short, there must be large temperature gradients present within the epithelia in order to result in fast conduction cooling. At the tissue surface, the amplitude of the temperature gradient is inversely proportional to the penetration depth. Therefore, the shorter the penetration depth, the faster the heat conduction and the shorter the ramp-down cooling phase. Consequently, lasers with a high absorption in water (see Fig. 3) and therefore with a low penetration depth (δ), are advantageous since they are capable of generating short-duration exposure times. In order to demonstrate these characteristics, Fig. 13 shows the calculated dependence of the duration of the temperature pulse at the tissue surface on the energy penetration depth,

for the energy pulse duration of t_{in} = 100 μs. The temperature evolution at the tissue surface was simulated using the numerical method as in [3, 11], for three energy penetration depths within the tissue, approximately representing Er:YAG ($\delta \approx 1$ μm), CO_2 ($\delta \approx 20$ μm) and near IR lasers in the range of 1.2-1.6 μm ($\delta \approx 400$ μm) [38-40]. An example of a laser with $\delta \approx 400$ μm is a 1,470 nm diode laser [32], however, this penetration depth can also be considered to approximately represent tissue resurfacing with radiofrequency (RF) [41] or ultrasound [42] energy-based devices that are typically characterized by even deeper energy penetration depths.

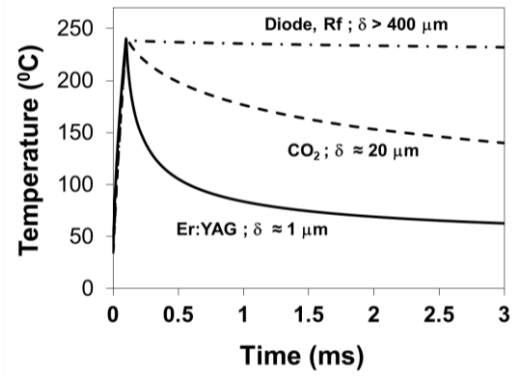

Fig. 13: The duration of thermal pulses for different penetration depths, δ. The pulse fluence was set to slightly below the threshold value as calculated for each of the three penetration depths. Note that for the shown penetration depth of 400 μm, the cooling phase extends significantly further than the presented time range.

The dependence of T_{crit} on the penetration depth and energy pulse duration can be seen in Fig. 14, which shows damage threshold temperatures as calculated using the VHS response model (Eq. 3) [11].

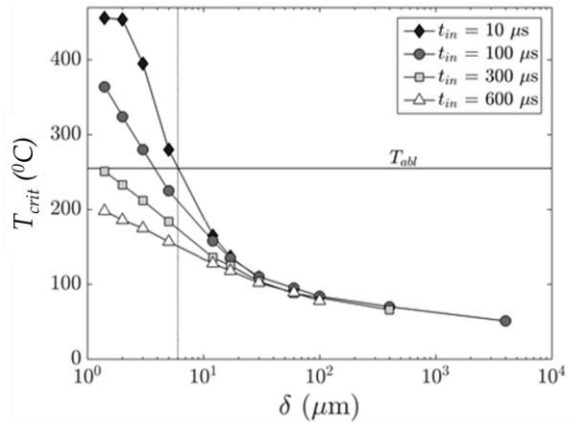

Fig. 14: Dependence of the critical temperature T_{crit} of the epithelial surface on the energy penetration depth δ, for different energy delivery times t_{in}. The optimal efficacy and safety window (denoted by the vertical line) lies within the range of parameters for an energy-based device, characterized by $T_{crit} < T_{abl}$.

As demonstrated by Fig. 14, the damage threshold temperatures are much higher than the normally assumed safe temperatures of up to about 65 ^{0}C [34], providing that the tissue is exposed to sufficiently short energy pulses, characterized by an extremely short penetration depth (δ).

The influence of the penetration depth on tissue damage can be seen on an example of skin resurfacing. Figure 15 shows the clinical effect on the skin following a single pulse with a 2,940 nm Er:YAG laser ($\delta \approx 1$ μm) or with 1,340 nm Nd:YAP laser ($\delta \approx$ 400-800 μm) [11]. The maximal skin surface temperature at the end of the laser pulse of $T_{max} \approx 250$ ^{0}C was the same for both laser wavelengths.

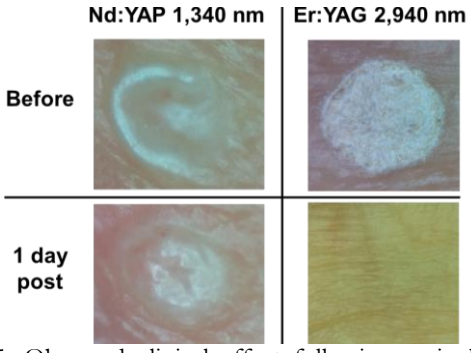

Fig. 15: Observed clinical effect following a single pulse with 2,940 nm Er:YAG or 1,340 nm Nd:YAP laser, both with a laser pulse duration of t_{in} = 300 μs [11] .

As can be seen from this clinical example, the longer exposure time generated by the longer penetration depth Nd:YAP laser resulted in a significantly higher damage to the tissue, in spite of the same maximal skin surface temperature.

It is these short thermal pulses that can be safely delivered to the epithelium using the extremely short penetration Er:YAG laser, that represent the additional mechanism of action explaining the reported extraordinary clinical effects of the Er:YAG laser with non-ablative resurfacing. This additional, indirect tissue regeneration mechanism is complementary to the direct stimulation of fibroblasts. The mechanism is based on triggering the stimulating signal transduction processes for transcription factor activation, gene expression and fibroblast growth, thus leading to new collagen and extracellular matrix formation. Namely, it is not only fibroblasts, but also the superficially located keratinocytes that are involved in the wound healing process. It is known that keratinocytes recruit, stimulate, and coordinate the actions of multiple cell types involved in healing [45-45]. In particular, keratinocytes and fibroblasts communicate with each other via double paracrine signaling loops, known as cross talk or dynamic reciprocity, that coordinate their actions to

restore normal tissue homeostasis after wounding [45]. In response to paracrine signaling from keratinocytes and inflammatory cells, fibroblasts synthesize collagen and promote cross-linking to form an extracellular matrix. In addition, the recent discovery of an "interstitium" [88] indicates that submucosa is not a wall of dense connective tissue, but consists of a previously unappreciated fluid-filled interstitial space, which may provide a very effective conduit for pro-fibrogenic signaling molecules.

Furthermore, it has been proposed that a controlled generation of reactive oxygen species (ROS) at very high local temperatures within the shallow penetration depth of the Er:YAG laser may provide an additional explanation for the observed healing effects exerted by the Er:YAG laser during rejuvenation treatments [51, 52]. Namely, low amounts of ROS have been found to stimulate wound healing via increased proliferation of keratinocytes and fibroblasts, which in turn generate collagen [53-55]. Furthermore, the generation of ROS during resurfacing procedures has been found to be enhanced by the unique 2,940 nm Er:YAG laser wavelength, which matches the exact vibrational oxygen-hydrogen (OH) stretch frequency of water, resulting in a resonant splitting of water molecules at high local temperatures [52].

The fast-pulsed heating can stimulate DNA expression and RNA for heat shock proteins (HSP), while not killing the cells by direct injury [46-47]. The HSP proteins are presumed to initiate temporary changes in cellular metabolism, resulting in the release and production of growth factors and thus in the increase of the rate of cell proliferation [48-50]. It should be noted that the shorter the penetration depth, the higher heat shock protein-synthesizing thermal pulses that can be generated without causing cell death. Out of all laser types, the Er:YAG laser allows delivery of the most intense heat shock-generating thermal pulses. For illustration, Fig. 16 shows, for different laser types, the exemplary maximal safe heat shock temperature elevations $\Delta T = T_{max} - T_0$, characterized by the maximal temperature T_{max} being bellow the critical temperature for cell injury.

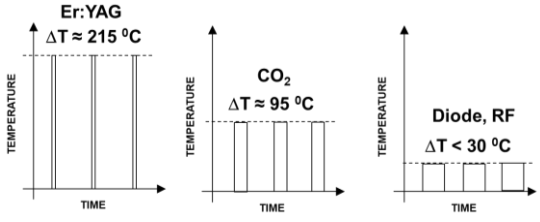

Fig. 16: Illustrative example of the dependence of the maximal heat-shock safe temperature elevations on the laser type. The depicted safe heat-shock temperature elevations are for $t_{in} \approx$ 100 -300 μs.

In addition, for laser wavelengths with extremely short penetration depths, such as the 2,940 nm wavelength of the Er:YAG laser, a safety window of laser pulse durations characterized by $T_{abl} < T_{crit}$, exists within which the critical temperature cannot be exceeded regardless of the laser pulse fluence delivered to the tissue. This characteristic potentially makes this type of device extremely safe for tissue resurfacing, since once the epithelia temperature reaches T_{abl}, the onset of minimally invasive, micron layer-by-layer ablation (see Fig. 2) automatically prevents the epithelium surface temperature from getting heated above $T_{abl} < T_{crit}$. As can be seen from Fig. 14, the longest penetration depth of an energy-based device for which the safety window exists for a reasonably long energy pulse is $\delta \leq 7$ μm, a condition that is fulfilled only by the Er:YAG laser wavelength.

d) Analysis of FotonaSmooth® mode repetitive irradiation

Figure 17 shows a typical temporal evolution of a tissue surface temperature T during and following a FotonaSmooth® mode, repetitive irradiation with N = 6 Er:YAG laser pulses at a repetition rate of 20 Hz.

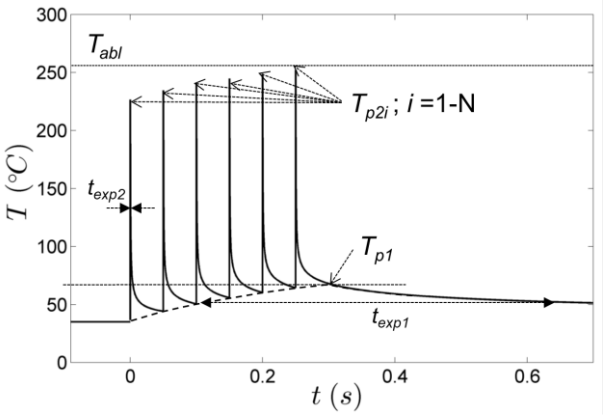

Fig. 17: Temporal evolution of surface temperature during and following FotonaSmooth® mode Er:YAG laser delivery.

We characterize the FotonaSmooth® mode temporal evolution by two types of peak temperatures: i) "fast" temperature peaks T_{p2i}, belonging to individual Er:YAG laser pulses i (with i = 1 to N) within the sequence of N pulses; and ii) "slow" temperature peaks T_{p1} defining the maximal temperature of the thermal "pulse" belonging to the long-duration rise and decay of the base-line temperature.

The evolution of the temperature deeper within the tissue during and following a FotonaSmooth® mode, repetitive irradiation with i = 1 – 20 pulses is depicted in Fig. 18. As can be seen from this figure, the long exposure temperature elevations (lasting several seconds) extend down to the depth (z) of several

hundred microns into the tissue.

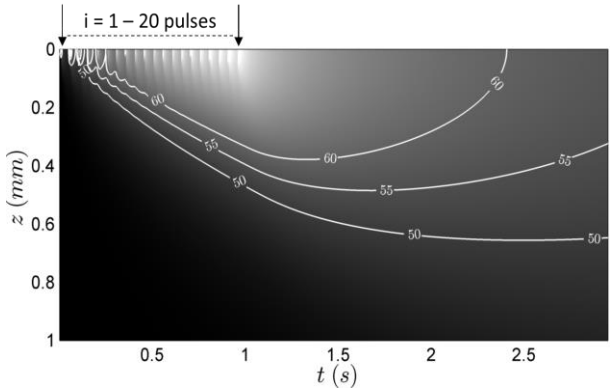

Fig. 18: Temporal evolution of deeper tissue temperatures during and following FotonaSmooth® mode Er:YAG laser delivery.

Roughly speaking, the tissue injury defined by T_{p1} can be due to the long exposure time t_{exp1}, considered to be determined primarily by the long exposure process 1, while the tissue injury defined by T_{p2i} , and characterized by the short exposure time t_{exp2} is determined primarily by the characteristics of the short exposure process 2. In order to avoid excessive tissue damage, the laser parameters should be chosen such that the short duration temperature peaks T_{p2i} are below the short exposure critical temperature T_{crit2}, and the long duration temperature peak T_{p1} is below the long exposure critical temperature T_{crit1} (See Fig. 19).

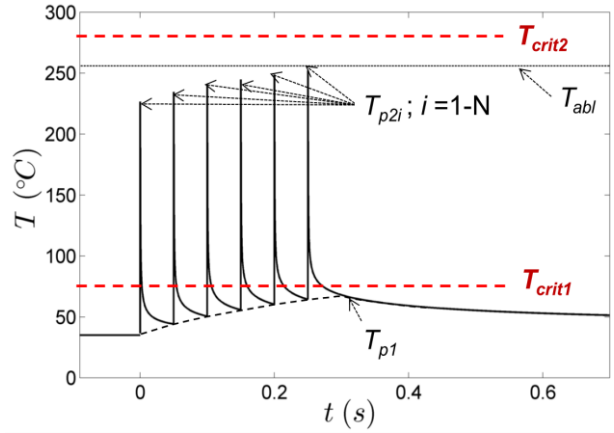

Fig. 19: Dual tissue remodeling is possible with the FotonaSmooth® mode Er:YAG laser because it allows the laser parameters to be adjusted such that both the short exposure temperature peaks T_{p2i} and the long exposure temperature peak T_{p1} are below their respective critical temperatures for excessive tissue injury, T_{crit2} and T_{crit1}.

As described earlier, the Er:YAG laser wavelength is absorbed within extremely short penetration depths, resulting in extremely short temperatures peaks T_{p2i}, characterized by a very high critical temperature T_{crit2}. Under appropriate conditions the short exposure critical temperature T_{crit2} is above the ablation temperature T_{abl}, providing the ultimate short-exposure safety since in case of the laser overdose, the on-set of laser ablation will prevent the short exposure process temperature peaks T_{p2i} to exceed the critical temperature T_{crit2}.

A similar conclusion can be made also for the long exposure temperature peak T_{p1} (See Fig. 20).

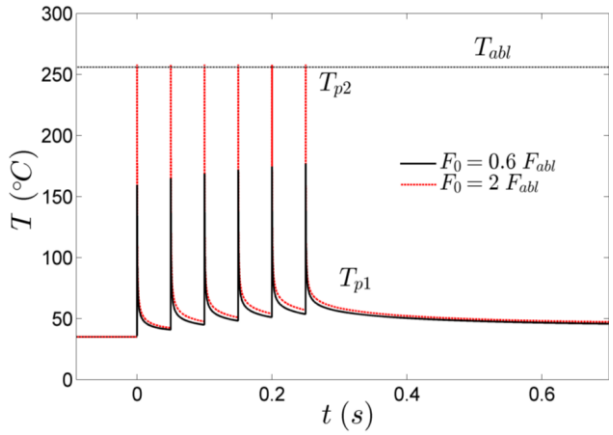

Fig. 20: For high Er:YAG laser fluences, the onset of ablation prevents further temperature rise, limiting the short-exposure temperature T_{p2} to T_{abl}. This also limits the increase of the long-exposure temperature peak T_{p1}, as can be seen from the very small difference between long exposure temperatures T_{p1} at a below-threshold single micro-pulse fluence of F_0 = 0.6 F_{abl} (black line) and at an above-threshold fluence of F_0 = 2 F_{abl} (red line).

As soon as the short exposure temperature peaks reach T_{abl}, the ablation process prevents further temperature growth, limiting the maximal short exposure temperature T_{max2} to T_{abl}. This also limits the growth of the long exposure temperature T_{p1} to a maximal temperature T_{max}, which depends only on the number of micro-pulses (N) and not on the single-pulse fluence F_0 or the cumulative fluence F_{SMOOTH} (See Fig. 21).

As can be concluded from Fig. 21, the base-line peak temperature, and resulting tissue injury, can be "digitally" controlled by adjusting the number of pulses (*N*) in the FotonaSmooth® sequence.

The dependence of the maximal long exposure temperature on the laser penetration depth can be seen in Fig. 22. As can be seen from this figure, the maximal long exposure temperature is higher for larger optical penetration depths. It is only for the Er:YAG laser's extremely short optical penetration depth of $\delta \approx 1$ μm that the maximal temperature T_{max1} is below the long-exposure critical temperature T_{crit1}.

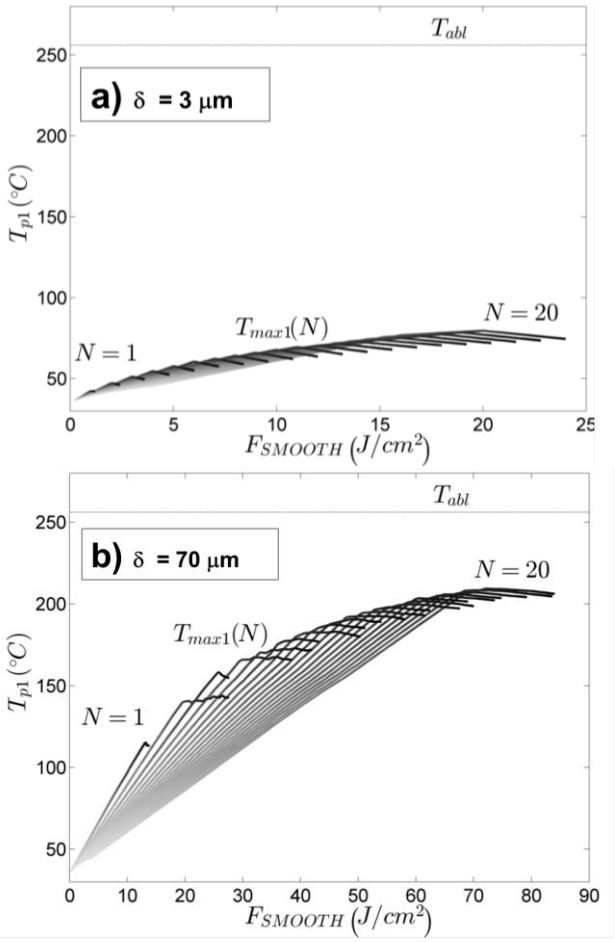

Fig. 21: Dependence of the long-exposure temperature peak on the cumulative fluence F_{SMOOTH} and number of micropulses (N) for δ = 3 μm and 70 μm. The micro-pulse frequency is f = 10 Hz. The shorter the optical penetration depth, the lower the maximal temperature at the tissue surface.

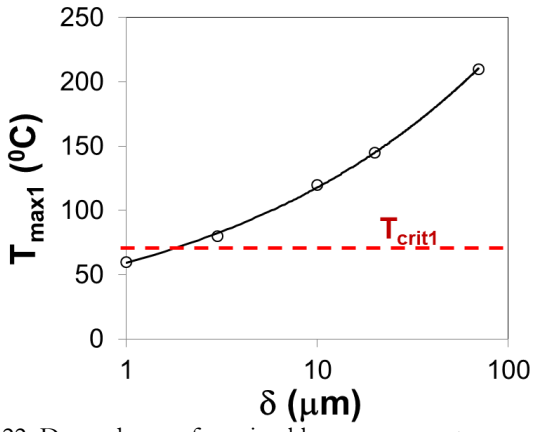

Fig. 22: Dependence of maximal long-exposure temperature T_{max1} on energy penetration depth δ for f = 10 Hz. For the Er:YAG laser's optical penetration depth $\delta \approx 1$ μm, the maximal temperature is below the long-exposure critical temperature T_{crit1}.

The above safety feature is especially relevant for the case of treating body cavities such as the vagina, with an internal wall surface not regularly shaped. Therefore the delivered fluence and consequently the generated heat uncontrollably vary from one location to another. There is also the accepted ± 20% variation in laser energy according to medical laser standards. Also, the energy source may not always be kept at the optimal distance or optimal angle with regard to the tissue surface, again resulting in non-uniform heat generation (see Fig. 23). And finally, human error can also occur. In all these cases, the Er:YAG laser ablation mechanism combined with the variable heat shock (VHS) dynamics protect the patient from any irreversible injury and keep the treatment within the safe resurfacing limits.

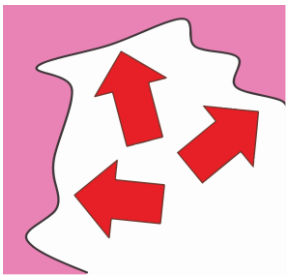

Fig. 23: The self-regulating feature of Er:YAG resurfacing is especially important when treating irregularly shaped surfaces, for example of a vaginal wall, where the angle of the laser beam with respect to the surface, and therefore the laser fluence, uncontrollably vary from one location to another.

IV. DISCUSSION

The superficial heat shocking involved in the dual tissue-remodeling mechanism (DTR) resembles the effects of the micro-needling technique, which aims not to injure keratinocytes but to stimulate them with superficial punctures and without any injury to fibroblasts [56, 57]. Similarly to laser resurfacing, the mechanism of action of micro-needling appears to involve not only a direct inflammatory response to the localized "ablation", but also indirectly induced cell proliferation by electrical signals [57]. Since with micro-needling only a relatively small percentage of the skin is being affected, the treatment outcome is expected to be accordingly limited. On the other hand, the FotonaSmooth® Er:YAG laser-induced thermal triggering mechanism can be viewed as non-ablative thermal "needling" (i.e., triggering) of the total treated skin surface, with the action of the spatially sharp needles being replaced by the action of temporarily "sharp" but spatially extended heat shock pulses. The extremely short thermal pulses which can be safely delivered to the epithelium using Er:YAG laser radiation represent an additional, indirect mechanism of action for regenerating epithelial and deeper lying connective tissues, which is complementary to the conventional direct slow stimulation of fibroblasts (See Fig. 24).

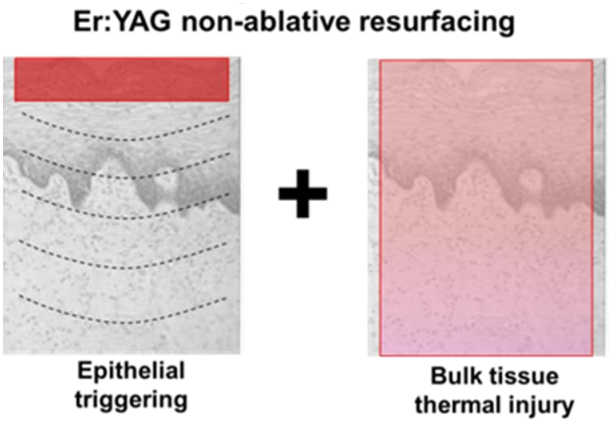

Fig. 24: Dual tissue-remodeling mechanism (DTR) involved in non-ablative resurfacing with FotonaSmooth® mode Er:YAG laser.

As shown above, the requirements for superficial heat shocking limit the range of "DTR" energy-based devices to short-pulsed lasers with appropriately short penetration depths within the tissue. Other types of energy-based devices, such as radiofrequency [41, 58] or ultrasound devices [42], have too long energy delivery times and extremely deep penetration depths, and are therefore not suitable for epithelial heat shock triggering. The requirement for the penetration depth to be below about 6 μm further narrows the choice of energy devices primarily to lasers with a wavelength positioned close to the water absorption peak at 2,940 nm. The Er:YAG laser thus appears to hold a very unique position within the group of resurfacing devices. We believe that this explains the reported safety and efficacy of FotonaSmooth® Er:YAG lasers when used for ablative or non-ablative resurfacing.

When considering the next most highly absorbed laser, i.e., the CO_2 laser, it can be concluded that the critical temperature for this type of laser is about 130 ^{0}C (See Figs. 13 and 15), which is much lower than the ablation temperature of $T_{abl} \approx 250\ ^0$C. Therefore, for the CO_2 laser wavelength the safety window is much narrower in comparison with the Er:YAG, making complication-free CO_2 ablative or non-ablative resurfacing procedures much more demanding to perform. This may explain why longer recovery times and a higher occurrence of complications have been reported for CO_2 laser resurfacing in comparison to Er:YAG resurfacing [59]. It may also explain why most of the CO_2 and other types of laser resurfacing procedures are performed in the ablative fractionated manner [60], where only a small percentage of the treated area is being irradiated, similarly to the needling technique. Further studies are needed to evaluate whether the fractionated ablative resurfacing of only a very small percentage of the treated area can be as effective and safe as the non-ablative full-spot, dual-mechanism regeneration procedure available with the Er:YAG laser wavelength. This question is particularly relevant since vaginal resurfacing procedures are being considered to be used as a regular (once every several years) maintenance protocol to prevent or slow down the symptoms of aging. Since it is known that repeated ablative wounding may cause scarring, non-ablative full-beam resurfacing appears to provide additional safety in this regard.

The regenerative effect of the FotonaSmooth® mode Er:YAG laser when used for minimally invasive, non-ablative resurfacing of the vaginal wall has been demonstrated in numerous clinical studies [8, 34, 61-62]. In a study by Lapii et al. [61], vaginal biopsy specimens after Er:YAG laser exposure showed signs of neocollagenesis and elastogenesis, foci of neoangiogenesis, reduction of epithelial degeneration and atrophy, and an increase of the fibroblast population. Morphometry showed that the volume density of blood capillaries and the thickness of the epithelial layer increased by 61.1% and 64.5%, respectively. In another study by Gaspar et al. [62], histological examination showed changes in the tropism of the vaginal mucosa and also angiogenesis, congestion, and restructuring of the lamina propria. Similarly, in a study by Bezmenko et al. [63], marked histological changes were observed, demonstrating an increase in the quantity and activity of fibroblasts as well as increased density of connective tissue and the emergence of neoangiogenesis.

Furthermore, the rejuvenation of mucous tissue following FotonaSmooth® mode Er:YAG non-ablative vaginal resurfacing has been shown to improve clinical symptoms of the following indications that are already cleared for marketing and sale in the EU, but have not yet been specifically cleared for promotion in the USA: vaginal atrophy [65-70], stress urinary incontinence (SUI) [17, 71-81], vaginal relaxation syndrome (VRS) [81-84] and pelvic organ prolapse (POP) [81-83].

As measured by ICIQ-SF, Pardo et al. [79], reported an improvement of SUI symptoms after non-ablative FotonaSmooth® Er:YAG resurfacing of vaginal mucosa in 79% of women. This data is in accordance with the study by Ogrinc et al. [78], which showed an improvement in 77% of women. Furthermore, Pardo et al. also show a complete reduction of SUI symptoms in 38.1% of women. Using pad testing, Tien et al. showed a complete reduction of SUI symptoms in 39% of women with very mild and 50% with moderate urine leakage. Furthermore, a significant improvement was noted in

39% with mild, 27.8% with moderate, and 60% (n=6) women with severe urine leakage. Non-ablative FotonaSmooth® Er:YAG resurfacing of the vaginal mucosa also resulted in improved sexual gratification for 81.8% of women according to Pardo et al. [79], which is supported by the study from Tien et al. Additionally, Tien et al. [80] show that 40% of the partners also reported improved sexual function 6 months after their female partners underwent the laser treatment. Assessed by a questionnaire addressing quality of life and the 1-h pad test, the severity of urine leakage decreased significantly also for women suffering from SUI type III (intrinsic sphincter deficiency) as shown by Gaspar et al. [72].

In two independent studies, Gambacciani et al. [68, 69] showed a statistically significant decrease of visual analogue scale (VAS) for dryness and dyspareunia with a statistically significant increase of Vaginal Health Index Score (VHIS) in women suffering from genitourinary syndrome of menopause (either because of the onset of menopause or from standard estrogen blocker therapy for breast cancer survivors). Similar results were obtained also by Bojanini et al [65].

In their study Gaviria et al. [83], showed that non-ablative FotonaSmooth® Er:YAG resurfacing results in a significant improvement of the vaginal tightness in 95% of women. Women also reported better sexual gratification after the treatment and 85% of their partners reported a significant improvement. Patients suffering from stress urinary incontinence (SUI) and pelvic organ prolapse (POP) also reported complete or partial improvement of their conditions. Similar results were obtained in a 3-year follow up study by Gaviria et al. [84]. Results on the improvement in POP were also demonstrated by another independent study by Ogrinc et al. [85].

Finally, the FotonaSmooth® and PIANO® modes represent TightScultping's complete body contouring solution, which can be, depending on the type of patient and the goal of the treatment, used either individually [91-93] or in concert [89, 90] as a combined dual-wavelength procedure.

V. CONCLUSIONS

Aspects of soft-tissue resurfacing with the Er:YAG laser, representing the mid-IR laser with the highest absorption in tissue water, were examined from the viewpoint of the mechanism of actions involved in FotonaSmooth® mode Er:YAG laser non-ablative resurfacing of skin during body sculpting procedures [89-93], of the vaginal wall to stimulate a healing response [61-87], of the oral tissue during thermotherapy of snoring and sleep apnea [9, 94-103], and of the correction of nasolabial folds wrinkle using intraoral (4D) non-ablative resurfacing [104].

It was shown that the unique, extremely short optical penetration depth of the Er:YAG wavelength makes this laser not only optimal for ablative procedures but also for non-ablative resurfacing.

Three unique features of the FotonaSmooth® mode Er:YAG laser, when used for non-ablative resurfacing, were demonstrated:

i) Dual tissue-regeneration mechanism (DTR)
ii) The unique safety of short-exposure superficial heat shocks
iii) The unique safety of long-thermal-exposure deep-tissue remodeling

The additional, indirect mechanism of action for regenerating epithelial and deeper lying connective tissues, which is facilitated by the safe delivery of extremely short Er:YAG thermal pulses to the epithelium is complementary to the conventional direct slow stimulation of fibroblasts This indirect mechanism of action is based on triggering stimulating signal transduction processes for transcription factor activation, gene expression and fibroblast growth, thus leading to new collagen and extracellular matrix formation.

The requirements for the dual tissue-remodeling mechanism limit the range of suitable energy-based devices to short-pulsed lasers with appropriately short penetration depths within the tissue. Other types of energy-based devices, such as radiofrequency or ultrasound devices, have large energy penetration depths into the tissue and are therefore not suitable for the fast epithelial heat-shock triggering involved in DTR. The requirement for the penetration depth to be below about 6 μm further narrows the choice of energy devices primarily to lasers with a wavelength positioned close to the water absorption peak at 2,940 nm. The FotonaSmooth® Er:YAG laser thus appears to hold a very unique position within the group of resurfacing devices. Analysis shows that thermotherapy using the FotonaSmooth® mode Er:YAG laser involves not only the additional fast heat-shocking mechanism of tissue regeneration, but also includes a unique self-regulating safety feature. These extraordinary DTR characteristics of the FotonaSmooth® Er:YAG laser may explain the reported safety and efficacy of FotonaSmooth® Er:YAG lasers when used for non-ablative skin tightening[89-93], thermotherapy of the vaginal wall to alleviate genitourinary syndromes of menopause [61-87], and for thermotherapy of snoring and sleep apnea [9, 94 -103].

NOTES

The authors acknowledge financial support from the state budget of the Ministry of Education, Science and Sport of Slovenia and the European Regional Development Fund (Project GOSTOP). Two of the authors (ML and FB) are affiliated also with Fotona d.o.o., Ljubljana, Slovenia.

REFERENCES

1. Alexiades-Armenakas MR, Dover JS, Arndt KA, The spectrum of laser skin resurfacing: Nonablative, fractional, and ablative laser resurfacing (2008) J Am Acad Dermatol, 58(5):719-737.
2. Lukac M, Perhavec T, Nemes K, Ahcan A (2010) Ablation and Thermal Depths in VSP Er:YAG Laser Skin Resurfacing. J LA&HA, J Laser and Health academy 2010(1): 56-71.
3. Majaron B, Plestenjak P, Lukac M (1999), Thermo-mechanical laser ablation of soft biological tissue: modeling the micro-explosions. Appl. Phys. B 69, 71–80
4. Majaron B, Sustercic D, Lukac M, Skaleric U, Funduk N (1998) Heat diffusion and debris screening in Er:YAG laser ablation of hard biological tissues. Appl Phys B 66:479-487.
5. Khatri KA, Ross V, Grevelink JM (1999) Comparison of Erbium:YAG and Carbon Dioxide Lasers in Resurfacing of Facial Rhytides. Arch Dermatol 135(4): 391-397.
6. Lukac M Ph.D., Sult T, Sult R (2007) New Options and Treatment Strategies with the VSP Erbium YAG Aesthetics Lasers; J LA&HA, J Laser and Health Academy 2007(1): 1-9.
7. Drnovsek Olup B, Beltram M, Pizem J (2004) Repetitive Er:YAG laser irradiation of human skin: A histological evaluation. Lasers in Surg Med 35:146–151
8. Vizintin Z, Lukac M, Kazic M, Tettamanti M (2015) Erbium laser in gynecology, Climacteric 18(1): 4-8
9. Storchi IF, Parker S, Bovis F, Benedicenti S, Amaroli A (2018) Outpatient erbium:YAG (2940 nm) laser treatment for snoring: a prospective study on 40 patients. Lasers Med Sci, published online Jan 15, 2018.
10. Ebrahim HM, Gharib K (2018) Correction of nasolabial folds wrinkle using intraoral non-ablative Er:YAG laser. J. Cosmet Laser Ther; DOI:10.1080/14764172.2018.1439964
11. Lukac M, Lozar A, Perhavec T, Bajd F, Variable heat shock response model for medical laser procedures, submitted to Lasers Med Sci, https://doi.org/10.1007/s10103-018-02704-1.
12. Nemes K, Diaci J, Ahcan U, Marini L, Matjaz Lukac (2014) Dependence of Skin Ablation Depths on Er:YAG Laser Fluence, J LA&HA, J Laser and Health Academy. 2014(1): 7-13
13. Fotona Smooth® is a registered trade mark of Fotona d.o.o.
14. Walsh JT, Deutsch TF (1989) Er:YAG laser ablation of tissue: measurement of ablation rates. Lasers Surg. Med. 9: 327 -37
15. Hibst R, Kaufmann R (1991) Effects of laser parameters on pulsed Er:YAG laser skin ablation. Lasers Med. Sci. 6(4): 391-397.
16. US FDA 510(k) clearance K143723.
17. Moritz AR, Henriques FC (1947) Studies of thermal injury, 2. The relative importance of time and surface temperature in the causation of burns. A J Pathol 23:695–720
18. Chen B et al (2008) Histological and Modeling Study of Skin Thermal Injury to 2.0 μm Laser Irradiation Lasers in Surgery and Medicine 40:358–370
19. Henriques FC, Moritz AR (1947) Studies of thermal injury, 1. The conduction of heat to and through skin and the temperature attained therein. A theoretical and an experimental investigation. A J Pathol 23:531–549
20. Ganceviciene R et al (2012) Skin anti-aging strategies. Dermatoendocrinol. 4(3): 308–319.
21. Gaspar A, Brandi H, Gomez V, Luque D (2016) Efficacy of Erbium:YAG Laser Treatment Compared to Topical Estriol Treatment for Symptoms of Genitourinary Syndrome of Menopause, Laser Surg Med. 49(2):160-168. doi: 10.1002/lsm.22569.
22. Johnson FH, Eyring H, and Stover BJ (1974) The Theory of Rate Processes in Biology and Medicine. Wiley, New York.
23. Wright NT (2003) On a relationship between the Arrhenius parameters from thermal damage studies. Journal of biomechanical engineering 125(2):300–304.
24. Weaver JA, Stoll AM (1967). NADC Memo Report 6708. In. Johnsville, Pennsylvania: United Stated Naval Air Development Center.
25. Beckham JT (2008) The role of heat shock protein 70 in laser irradiation and thermal preconditioning. PhD thesis, Faculty of the Graduate School of Vanderbilt University.
26. Takata AN (1974) Development of criterion for skin burns. Aerosp Med. 45:634–637
27. Wu YC (1982) A Modified Criterion for predicting thermal injury. Nat Bur Stand. In: Washington, District of Columbia.
28. Fugitt CE (1995) A rate process of thermal injury. Armed Forces Special Weapons Project No. AFSWP-606.
29. Gaylor DC (1989) Physical mechanism of celluar injury in electrical trauma. Ph.D. thesis Massachusetts Institute of Technology.
30. Simanovskii DM, Mackanos MA, Irani AR, O'Connell-Rodwell CE, Contag CH, Schwettman HA, and Palanker DV, Cellular tolerance to pulsed hyperthermia, Phys Rev E 74, 011915 (2006), doi: 10.1103/PhysRevE.74.011915.
31. Simanovskii D, Sarkar M, Irani A, O'Connell-Rodwell C, Contag C, Schwettman A, D. Palanker, Cellular tolerance to pulsed heating, Proc. of SPIE 5695, 254-259 (2005), doi: 10.1117/12.601774.
32. Pirnat S, Lukac M, Ihan A (2011) Thermal tolerance of E. faecalis to pulsed heating in the millisecond range. Lasers Med Sci (2011) 26:229–237
33. J. Kampmeier, B. Radt, R. Birngruber, R. Brinkman, Thermal and Biomechanical Parameters of Porcine Cornea., Cornea 19, 355, 2000: 355-363.
34. N. Fistonic, I. Fistonic, S Findri Gustek, I. Sorta Bilajac Turina, D. Franic, Z. Vizintin, M. Kazic, I. Hreljac, T. Perhavec, M. Lukac (2016) Minimally invasive, non-ablative Er:YAG laser treatment of stress urinary incontinence in women – a pilot study. Lasers Med Sci 31: 635-643
35. Majaron B, Srinivas SM, Huang HL, Nelson JS (2000) Deep coagulation of dermal collagen with repetitive Er:YAG laser irradiation. Lasers Surg. Med. 26:215–222
36. Majaron B, Kelly KM, Park HB (2001) Er:YAG Laser Skin Resurfacing Using Repetitive Long-Pulse Exposure and Cryogen Spray Cooling: I. Histological Study Lasers in Surgery and Medicine 28:121-130
37. Majaron B, Verkruysse W, Nelson S (2001) Er:YAG Laser Skin Resurfacing Using Repetitive Long-Pulse Exposure and Cryogen Spray Cooling: II. Theoretical Analysis. Lasers in Surgery and Medicine 28:131-137
38. Mordon S et al (2000) In Vivo Experimental Evaluation of Skin Remodeling by Using an Er:Glass Laser With Contact Cooling. Lasers Surg Med 27:1–9
39. Dodero D et al (2018) Solid State Vaginal Laser for the Treatment of Genitourinary Syndrome of Menopause: A Preliminary Report. Open Journal of Obstetrics and Gynecology 8: 113- 1210
40. Milanic M. Majaron B (2012) Energy deposition profile in human skin upon irradiation with a 1,342 nm Nd:YAP laser. Lasers in Surgery and Medicine 45:8–14
41. Millheiser LS, Pauls RN, Herbst SJ, Chen BH (2010) Radiofrequency treatment of vaginal laxity after vaginal delivery: Nonsurgical vaginal tightening. J Sex Med 7(9):3088–3095
42. Dirk Meyer-Rogge, Frank Rösken, Peter Holzschuh, Bruno D'hont, Ilja Kruglikov (2012) Facial Skin Rejuvenation with High Frequency Ultrasound: Multicentre Study of Dual-Frequency Ultrasound. Journal of Cosmetics, Dermatological Sciences and Applications. 2: 68-73
43. Bourke CD et al (2015) Epidermal keratinocytes initiate wound healing and pro-inflammatory immune responses following percutaneous schistosome infection International Journal for Parasitology 45: 215–224

44. Pastar I et al (2014) Epithelialization in wound healing: A comprehensive review. Advances in Wound Care. 3(7): 445-464
45. Wojtowicz AM et al (2014) The importance of both fibroblasts and keratinocytes in a bilayered living cellular construct used in wound healing Wound Rep Reg 22: 246–255.
46. Kumar,V, Abbas AK, Fausto N, and Mitchell RN. Robbins basic pathology. Saunders-Elsevier, Philadephia, 8th edition, pp. 1–224 (2007).
47. Alberts B, Johnson A, Lewis J et al. Molecular biology of the cell. Garland Science, New York, 4th edition, pp. 1–1463 (2002).
48. Bowman PD (1997) Survival of human epidermal keratinocytes after short-duration high temperature: synthesis of HSP70 and IL-8. Am J Physiol. ;272(6 Pt 1):C1988-94.
49. Capon A, Mordon S (2003) Can thermal lasers promote skin wound healing? Am J Clin Dermatol 4 (1): 1-12
50. Mackanosa MA, Contag CH (2011) Pulse duration determines levels of Hsp70 induction in tissues following laser irradiation. J Biomed Opt 16(7), 078002 (July 2011)
51. Lubart R, Friedmann H, Lavie R, Baruchin A (2011) A novel explanation for the healing effect of the Er:YAG laser during skin rejuvenation. Journal of Cosmetic and Laser Therapy 13: 33–34
52. Lubart R, Kesler G, Lavie R, Friedmann H (2005) Er:YAG laser promotes gingival wound repair by photo-dissociating water molecules. Photomed Laser Surg. 2005 Aug;23(4):369-72.
53. Gordillo, G.M., and Sen, C.K. (2003) Revisiting the essential role of oxygen in wound healing. Am. J. Surg. 186, 259-263
54. Rojkind, M., Dominguez-Rosales, J.A., Nieto, N., and Green, P. (2002) Role of hydrogen peroxide and oxidative stress in healing responses. Cell. Mol. Life. Sci. 59,1872-1891
55. Burdon, R.H. (1995). Superoxide and hydrogen peroxide in relation to mammalian cell proliferation. Free Radic. Biol. Med. 18, 775-794.
56. Zhu H (2014) Acupoints Initiate the Healing Process. Medical Acupuncture, 26(5): 264-270
57. Horst Liebla, Luther C. Kloth (2013) Skin Cell Proliferation Stimulated by Microneedles. Journal of the American College of Clinical Wound Specialists 4(1): 2–6
58. Hardy LA et al (2016) Laser Treatment of Female Stress Urinary Incontinence: Optical, Thermal, and Tissue Damage Simulations. Proceedings Volume 9689, Photonic Therapeutics and Diagnostics XII; 96891R (2016)
59. Khatri KA, Ross V, Grevelink JM (1999) Comparison of Erbium:YAG and Carbon Dioxide Lasers in Resurfacing of Facial Rhytides. Arch Dermatol 135(4): 391-397.
60. N. Zerbinati, at al. (2015) Microscopic and ultrastructural modifications of postmenopausal atrophic vaginal mucosa after fractional carbon dioxide laser treatment. Lasers Med. Sci. 30(1): 429-436.
61. G.A. Lapii, A. Yu. Yakovleva, and A.I. Neimark (2017) Structural Reorganization of the Vaginal Mucosa in Stress Urinary Incontinence under Conditions of Er:YAG Laser Treatment, Bulletin of Experimental Biology and Medicine, Feb Vol.162, No.10:510-514.
62. A. Gaspar, H.Brandi, V. Gomez, D. Luque (2016) Efficacy of Erbium:YAG Laser Treatment Compared to Topical Estriol Treatment for Symptoms of Genitourinary Syndrome of Menopause, Laser Surg Med. 49(2):160-168. doi: 10.1002/lsm.22569.
63. Bezmenko A.A. et al. (2014) Morphological substantiation of applying the Er:YAG laser for the treatment of stress urinary incontinence in women, Journal of Obstetrics and Women Diseases, 63(3):21-25.
64. I.A. Kulikov, L.B. Spokoinyi, E.A. Gorbunova,.I.A. Apolikhina (2017) A Method For Photothermal Tissue Reconstruction Using ErYAG Laser Fotona in Modern Gynecology, Akusherstvo i Ginekologiya / Obstertics and Gynecology, (11): 160-167.
65. J.F. Bojanini B., A. M. Mejía C., Laser Treatment of Vaginal Atrophy in Post-menopause and Post-gynecological Cancer Patients, J Laser and Health Academy (2014) No.1, 65-71.
66. Gambacciani M. et al., Short term effect of Vaginal Erbium Laser on the Genitourinary Syndrome of Menopause, Minerva Ginecologica (2015).
67. Gambacciani M., Levancini M., Vaginal Erbium Laser: the Second Generation Thermotherapy for the Genitourinary Syndrome of Menopause (GSM) in Breast Cancer Survivors. A preliminary report of a pilot study – Italian Jorunal of Gynecology and Obstetrics, 27:N1 (2015).
68. Gambacciani M., Levancini M, Cervini M., Vaginal erbium laser: the second-generation thermotherapy for the genitourinary syndrome of menopause, Climacteric (2015); 18:1-7.
69. M.Gambacciani, M. Levancini, Vaginal erbium laser as second-generation thermotherapy for the genitourinary syndrome of menopause: a pilot study in breast cancer survivors, Menopause: The Journal of The North American Menopause Society. 24(3):316-319.
70. M.Gambacciani, S. Palacios, Laser therapy for the restoration of vaginal function, Maturitas 99 , 10–15 (2017).
71. Fistonic I., et al., Minimally invasive laser procedure for early stages of stress urinary incontinence (SUI), J Laser and Health Academy, No.1. (2012).
72. A. Gaspar, H. Brandi, Non-ablative erbium YAG laser for the treatment of type III stress urinary incontinence (intrinsic sphincter deficiency), Journal of Laser in Medical Science, 2017, Apr;32(3):685-691 (2017).
73. Bezmenko A.A. et al., Treatment of stress urinary incontinence with Er:YAG laser: some biochemical parameters of connective tissue metabolism, Journal of Experimental and Clinical Urology (2014).
74. Bezmenko A.A. et al., Conservative ways of urinary stress incontinence treatment, Journal of Russian Military Medical Academy (2014).
75. Gambacciani M. et al (2015), Rationale and design for the Vaginal Erbium Laser Academy Study (VELAS): an international multicenter observational study on genitourinary syndrome of menopause and stress urinary incontinence, Climacteric. 18:sup1, 43-48.
76. N. Fistonic, I. Fistonic, A. Lukanovic, S. Findri-Gustek, I. Sorta Bilajac Turina, D. Franic, First assessment of short term efficacy of Er:YAG laser treatment on stress urinary incontinence in women: prospective cohort study, Climacteric (2015), 18:sup1, 37-42.
77. M.M.Khalafalla, A:M: Elbiaa, I.A.Abdelazim, M. Hussain, Minimal Invasive Laser Treatment for Female Stress Urinary Incontinence, Obst&Gyn Int. Journal (2015) 2(2) 00035.
78. U.B. Ogrinc, S. Sencar, H. Lenasi, Novel Minimally Invasive Laser Treatment of Urinary Incontinence in Women, Laser in Surgery and Medicine (2015).
79. J.Pardo, V. Sola, A. Morales, Treatment of female stress urinary incontinence with Erbium YAG laser in non-ablative mode, European Journal of Obstetrics, Gynecology and Reproductive Biology, 204 (2016) 1-4.
80. YW. Tien, SM. Hsiao, CN. Lee, HH.Lin (2016) Effects of laser procedure for female urodynamic stress incontinence on pad weight, urodynamics, and sexual function, Int Urogynecol J, DOI 10.1007/s00192-016-3129-y (2016).
81. M.A. Barber, I. Eguiluz, Patient Satisfaction with Vaginal Erbium Laser Treatment of Stress Urinary Incontinence, Vaginal Relaxation Syndrome and Genito-urinary Syndrome of Menopause, J Laser and Health Academy No.1, 18-23, (2016).
82. J.I. Pardo, V.S. Dalenz, Laser Vaginal Tightening with Non-ablative Er:YAG for Vaginal Relaxation Syndrome. Evaluation of Patient Satisfaction, J Laser and Health Academy (2016) No.1, 12-17, (2016).
83. Gaviria J. et al., Laser Vaginal Tightening (LVT) – evaluation of a novel noninvasive laser treatment for vaginal relaxation syndrome, J Laser and Health Academy, No.1 (2012).
84. J. Gaviria, B. Korosec, J. Fernandez, G. Montero, Up to 3-year Follow-up of Patients with Vaginal Relaxation Syndrome Participating in Laser Vaginal Tightening, J Laser and Health Academy No.1, 6-11, (2016).
85. U.B. Ogrinc, S. Sencar (2017): Non-ablative vaginal erbium YAG laser for the treatment of cystocele, Italian Journal of Gynecology and Obstetrics, 29:N1 (2017).
86. N. Okui, Comparison of Erbium-YAG laser treatment with TVT and TOT in Asian women with SUI, Geriat. Med. 55(4), 421-423, 2017.

87. Yu.E. Dobrokhotova, I.Yu.Ilyina, M.G. Venedkitova, K.V. Morozova, V.A. Suvorova, S.A.Zalesskaya, ErYAG Laser Treatment for Genitourinary Disorders, Akusherstvo i Ginekologiya / Obstertics and Gynecology, 2017 (10): 84-91, (2017).
88. Benias PC (2018) Structure and Distribution of an Unrecognized Interstitium in Human Tissues. Scientific Reports 8:4947; DOI:10.1038/s41598-018-23062-6
89. Lukac M, Zorman A, Kukovic J, Bajd F (2018) TightSculpting®: A Complete Minimally Invasive Body Contouring Solution; Part II: Tightening with FotonaSmooth technology; J LA&HA - J Laser Health Acad; 2018(1):26-35.
90. Lukac M, Kukovic J, Tasic Muc B, Lukac N, Milanic M (2018) TightSculpting®: A Complete Minimally Invasive Body Contouring Solution; Part I: Sculpting with PIANO technology; J LA&HA - J Laser Health Acad; 2018(1):16-25.
91. Drnovsek Olup B, Beltram M, Pizem J (2004) Repetitive Er:YAG laser irradiation of human skin: A histological evaluation. Lasers in Surg Med 35:146–151.
92. Gaspar A (2013) Tightening of Facial Skin Using Intraoral 2940 nm Er:YAG SMOOTH Mode, J LA&HA - J Laser Health Acad 2013; 2013(2):17-20.
93. Lukac M, Perhavec T, Nemes K, Ahcan A (2010) Ablation and Thermal Depths in VSP Er:YAG Laser Skin Resurfacing. J LA&HA, J Laser and Health academy 2010(1): 56-71.
94. Sippus J (2015) CASE REPORT: NightLase® Procedure – Laser Snoring and Sleep Apnea Reduction Treatment; J LA&HA, J Laser and Health Academy 2015(1): 1-5
95. Jovanovic J (2011) NightLase™ - Laser-Assisted Snoring and Apnea Reduction, 9 Months of Experience (Summary); J LA&HA, J Laser and Health Academy 2011(1):S11
96. Dovsak D, Gabrijelcic J, Vizintin Z (2011) NightLase™ - A New Laser Treatment Method for the Reduction of Snoring and Sleep Apnea - A Pilot Study (Summary); J LA&HA, J Laser and Health Academy 2011(1):S09-S10.
97. Miracki K, Vizinti Z (2013) Nonsurgical Minimally Invasive Er:YAG Laser Snoring Treatment; J LA&HA, J Laser and Health Academy 2013(1):36-42
98. Svahnstrom K (2013) Er:YAG Laser Treatment of Sleep-Disordered Breathing; J LA&HA, J Laser and Health Academy 2013(2):13-16.
99. Unver T, Usumez A, Aytugar E, Kıran T (2015) Histological Effects of NightLase® in the Soft Palate of Rats: A Pilot Study; J LA&HA, J Laser and Health Academy 2015(1).
100. Pang J (2016) NightLase® Treatment for Sleep-Disordered Breathing; J LA&HA, J Laser and Health Academy 2016(1): S05.
101. Guimera JA (2015) Noninvasive Treatment of Snoring and Sleep Apnea with Erbium YAG Laser; J LA&HA, J Laser and Health Academy 2015(1): S16.
102. Janjic M (2018) NightLase® Smooth Mode Protocol; J LA&HA, J Laser and Health Academy 2018(1): CB01.
103. Ahnblad P (2017) Nasal Obstruction with Hypertrophic Inferior Turbinate: Treatment with Non-ablative Erbium YAG laser – a Pilot Study with Randomized Placebo-Controlled Trial Design; J LA&HA, J Laser and Health Academy 2017(1): 33-37.
104. Ebrahim HM, Gharib K (2018) Correction of nasolabial folds wrinkle using intraoral non-ablative Er:YAG laser, Journal of Cosmetic and Laser Therapy, DOI:10.1080/14764172.2018.1439964: 1-5.